Mikailalsys Journal of Advanced Engineering International

e-ISSN : 3046-9694
p-ISSN : 3046-8914

Index : Harvard, Boston, Sydney University, Dimensions, Lens, Scilit, Semantic, Google, etc

https://doi.org/10.58578/MJAEI.v2i3.7671

Hydrothermal Liquefaction of Mango Seed Kernel to Biocrude Oil and Hydrochar as a Precursor for Biofuel and Chemicals

A. M. Stone[1], K. Garba[2], M. B. Adamu[3], A. M. Hammari[4]
[1,2,3]Abubakar Tafawa Balewa University, Bauchi, Nigeria
[4]Gombe State University, Gombe, Nigeria
stoneamosm@gmail.com

Article Info:

Submitted:	Revised:	Accepted:	Published:
Oct 13, 2025	Nov 4, 2025	Nov 16, 2025	Nov 21, 2025

Abstract

As the global population grows and conventional resources are rapidly depleted, ensuring energy security and environmental sustainability requires the development of alternative energy sources. High-moisture food waste can be converted into valuable products through hydrothermal liquefaction (HTL), which offers an alternative to traditional waste treatment methods by processing biomass with high moisture content without prior drying, operating at 250–400 °C and 7–10 MPa to produce an energy-dense liquid fuel precursor known as bio-crude oil. This study investigates the thermal decomposition behavior of mango seed kernel (MSK) under batch HTL conditions. The MSK feedstock is characterized by a volatile matter content of 68.71% w/w, fixed carbon of 23.64% w/w, oxygen of 46.13% w/w on a dry basis, and a higher heating value (HHV) of 12.72 MJ/kg. Experiments were conducted at different temperatures (275, 300, and 325 °C) and reaction times (15, 30, and 45 min) at a constant biomass-to-water ratio of 1:7. The maximum bio-oil yield of 27.75 wt% was obtained at 300 °C for 30 min, with carboxylic acids/esters identified as the main compounds in both the light and heavy biocrude oil fractions. The

MJAEI Journal is licensed under a Creative Commons Attribution-NonCommercial-ShareAlike 4.0 International License

resulting hydrochar exhibited a high carbon content (75–81 wt%), moderate oxygen content (19–24 wt%), and trace amounts of K, Ca, Mg, and P, while FTIR analysis revealed a carbon-rich matrix with oxygenated functionalities (–OH, C=O, and C–O groups) together with aromatic C=C stretches. The study underscores the potential of MSK-derived bio-oil as a precursor for biofuels and biochemicals and highlights the need for further research on harnessing other HTL by-products, such as gases and aqueous organics, for biofuel, biochemical, and related applications.

Keywords: Hydrothermal Liquefaction; Mango Seed Kernel; Biocrude Oil; Biofuel Production; Biochemical Precursors; Hydrochar; Waste Valorization

INTRODUCTION

One of the greatest challenges nowadays is the maintainable administration of food waste. It has been reported by the Food and Agricultural Organization of the United Nations (UN) that one third of the food produced in the world for human consumption is been wasted (FAO et al., 2021). A fresh report of the United Nations regarding food wastage has revealed that food wastage in Nigeria per citizen is the highest in Africa (FAO, 2021). According to the report, a Nigerian waste at least 189 kilograms of food every year, amounting to a total of 37.9 million tons of food every twelve months (UNEP, 2021). These food wastes can be valorized in a number of ways. It can be composted, landfilled or incinerated. However, these ways emit greenhouse gases (CO_2, CH_4). Currently, effective methods of converting food waste into fuel have been developed which include biochemical and thermochemical conversion (Xuesong et al., 2023). The most common methods include pyrolysis, gasification and hydrothermal liquefaction. Biomass is converted to liquid and gaseous products at high temperatures and pressures in all of these methods (Romo, 2019).

Thermochemical and biochemical technologies can be used to process complex food wastes, mixtures that consist primarily of carbohydrates, proteins and oils, but also minor components including minerals and salts (Gu et al., 2019). Anaerobic digestion converts organic wastes into methane-rich biogas; however, digestion is a slow process, requiring large reactor volumes and yielding a product that must undergo significant upgrading for many applications (Cheng et al., 2020). When compared to digestion, gasification more rapidly converts organic wastes into a methane-rich syngas. Fast pyrolysis is the rapid thermal conversion of organic wastes or biomass to energy-rich oils. However, both gasification and

pyrolysis require dry feeds and the energy required to dry food waste detracts from the processes. Thermochemical processing via hydrothermal liquefaction (HTL) is an attractive process for food wastes, which is capable of converting a broad range of wet organic solids at moderate temperatures and high pressures without the need for a costly biomass drying step. HTL reactions are carried out at elevated temperatures (250–380°C) and pressures (7–30 MPa) in a hydrothermal water reaction medium for relatively short residence times (10–60 min) to form a carbon rich bio-oil phase along with an aqueous byproduct phase. HTL has been demonstrated for many organic-rich feeds and at a pilot plant scale of 2000 dry metric tons of waste per day (Maag et al., 2018).

Among these many techniques, hydrothermal liquefaction (HTL) looks promising as it requires a wet feedstock thereby eliminating the cost of drying the biomass. Products of HTL are bio-oil with high heating value and by-products in the gaseous, solid and liquid phases (Divyabharathi et al., 2022).

MATERIALS AND METHODS

Sample Collection and Preparation

Mango seed kernel was collected from Muda Lawal market, Bauchi, Bauchi State, Nigeria as the biomass feedstock for the hydrothermal liquefaction process. The bush mango or Irvingia gabonensis which is locally referred to as the "dan cameroon" is the specie of mango used as it is the mostly cultivated in the city and its environment. The sample was oven-dried at 100°C for 24 h, the dried sample was pulverised and sieved through a mesh to obtain a sample of sizes approximately 700 μm. Acetone and Dichloromethane were purchased from Chuzz Bond International, Jos-Nigeria. All chemicals and reagents were of analytical grade. Distilled water was obtained from Gubi Dam Water Treatment Plant Laboratory, Bauchi-Nigeria. Nitrogen gas was purchased from a local vendor, kaduna-Nigeria. Oven was used to dry the mango seed kernel (Manufactured by Ragaterm, Italy).

Biomass Characterization

Ultimate analysis was performed to determine the carbon (C), hydrogen (H), nitrogen (N) and Sulphur(S) content using a ThermoFisher Scientific Flash 2000 Organic Elemental Analyzer. A small amount (~5 mg) of solid samples (algae sample, model compounds solid residues; dried, particle size <60 μm) were placed inside small tin capsules

alongside a similar amount of vanadium pentoxide (V_2O_5) as a combustion booster during the analysis. All measurements were repeated in triplicate and the average values were reported. Oxygen (O) was calculated by difference.

The proximate analysis provides information on moisture, ash content, volatile matter and fixed carbon in MSK. Moisture content was determined according to AOAC (2000) at 105°C (Shen, 2024). The percentage moisture content was calculated using formular from Equation 1:

$$Moisture\ (\%) = \frac{Initial\ oven\ dry\ weight}{Initial\ weight} \times 100 \quad \ldots (1)$$

The Ash content was determined by weighing a known amount of dried sample cakes into a pre-weighed 25 cm^3 silica crucibles, then the crucible containing the samples were heated in a muffle furnace at 575°C for 3 hours and cooled in a desiccator, the formular for ash content calculation depicted in Equation 2 (Shen, 2024).

$$Ash\ (\%) = \frac{Weight\ of\ ash}{Weight\ of\ sample} \times 100 \quad \ldots (2)$$

The volatile matter was determined by placing known amount of sample into a pre-weighed crucible. The crucible containing the samples was heated in a muffle furnace at 950°C for 3 minutes then cooled in a desiccator (Gollakata et al., 2018). The percentage weight loss of the sample was calculated using Equation 3:

$$Volatile\ matter\ (\%) = \frac{Weight\ loss\ of\ dry\ sample}{Weight\ of\ dry\ sample} \times 100 \quad \ldots (3)$$

The fixed carbon is determined by subtracting 100 from the percentage volatile matter and ash content (Jiang et al., 2023). The formular for the determination of fixed carbon is depicted in Equation 4.

$$Fixed\ carbon\ (\%) = 100 - [volatile\ (\%) + ash\ (\%)] \quad \ldots (4)$$

To determine the HHV of MSK, bomb calorimetry is the standard method used. It provides an accurate measurement of the energy content in the sample. The HHV value can also be calculated using Dulong's formular in Equation 5. It is expressed in MJ/kg, it indicates the energy potential of the MSK as a biofuel.

$$HHV\left(\frac{MJ}{kg}\right) = 0.335C\% + 1.422\left(H\% - \frac{O\%}{8}\right) \quad \ldots (5)$$

The ultimate analysis conducted on the MSK is presented in Table 1. The result shows that the elemental composition of C, H, N, S and O from MSK are 46.133, 5.231, 1.212, 0.101 and 47.323 wt % respectively. Also, Table 1 shows that MSK has 68.71 wt% of volatile matter, 23.64 wt% of fixed carbon, 6.11 wt% of moisture content and 1.54 wt% of ash content.

Table 1: Properties of Mango seed Kernel from ultimate and proximate analysis

Property	
Proximate analysis	%w/w, dry basis
Moisture content	6.11
Volatile matter	68.71
Fixed carbon	23.64
Ash	1.54
Elemental composition	(%w/w, dry basis)
Carbon	46.133
Hydrogen	5.231
Nitrogen	1.212
Sulphur	0.101
Oxygen	47.323
HHV (MJ/kg)	12.72

Experimental Set-up

The HTL experiment was performed in a batch set-up, utilizing a 1 Liter reactor fabricated from stainless steel and its top body was firmly closed and covered with a bolted steel flange. The reactor cap includes a pressure gauge to record internal pressure. It is also equipped with a thermocouple. An air gasket was positioned between the cap and the autoclave body to ensure proper sealing. For heating, the reactor was equipped with a heating coil round about it at a heating rate of approximately 7.5°C per min. and it is being insulated to prevent heat loss to the environment. A controller was connected to the thermocouple to continuously monitor temperature during the reactor heating phase. As built diagram of the reactor set-up is shown in Plate 1. The MSK was weighed and loaded in the reactor at a fixed loading quantity of 40g. De-ionized water was added to the reactor on a biomass water ratio of 1:7 throughout the experiment. The mixture was stirred carefully to achieve homogeneity. The reactor was tightly closed and was purged 3 times with nitrogen to

remove oxygen that could induce ignition. Two variables were evaluated; reaction time and temperature. Times of 15, 30 and 45 mins were examined. The tested temperatures were 275°C, 300°C and 325°C. Table 2 presents the temperature and reaction time combinations tested for the biomass hydrothermal liquefaction. The reaction was initiated once the temperature of the mixture reached the set point. The pressure in the reactor was self-generated as the temperature increases

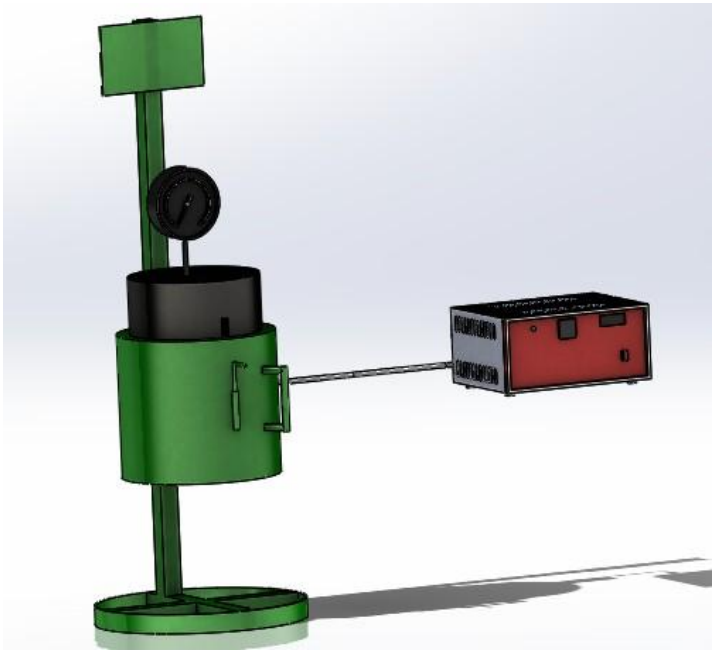


Plate 1: **Hydrothermal reactor set-up (As-built)**

Table 2: Temperature and reaction time combination of the hydrothermal liquefaction

ID	Temperature (°C)	Reaction time (min)
1.	275	15
2.	275	30
3.	275	45
4.	300	15
5.	300	30
6.	300	45
7.	325	15
8.	325	30
9.	325	45

Separation of products

Figure 1 shows how the HTL products will be collected and separated according to the mass balance of the products. After the HTL reaction, the reactor was then allowed to cool naturally. Gases were then vented off and the reactor was unbolted. The solid-liquid mixture was centrifuged at 3000rpm for 10 mins to separate the liquid and solid products. The solid was washed with acetone until the washing solution became colorless. The acetone soluble fraction was evaporated and the remaining fraction was labelled as heavy bio-crude (HBC) fraction. The solid remaining is known as the hydro char. An equal quantity of dichloromethane (DCM) was added to the liquid and centrifuged at 3000rpm for 10 mins. The mixture formed three layers of DCM, the bio-crude called light bio-crude (LBC) and the aqueous phase which can easily be separated by decanting.

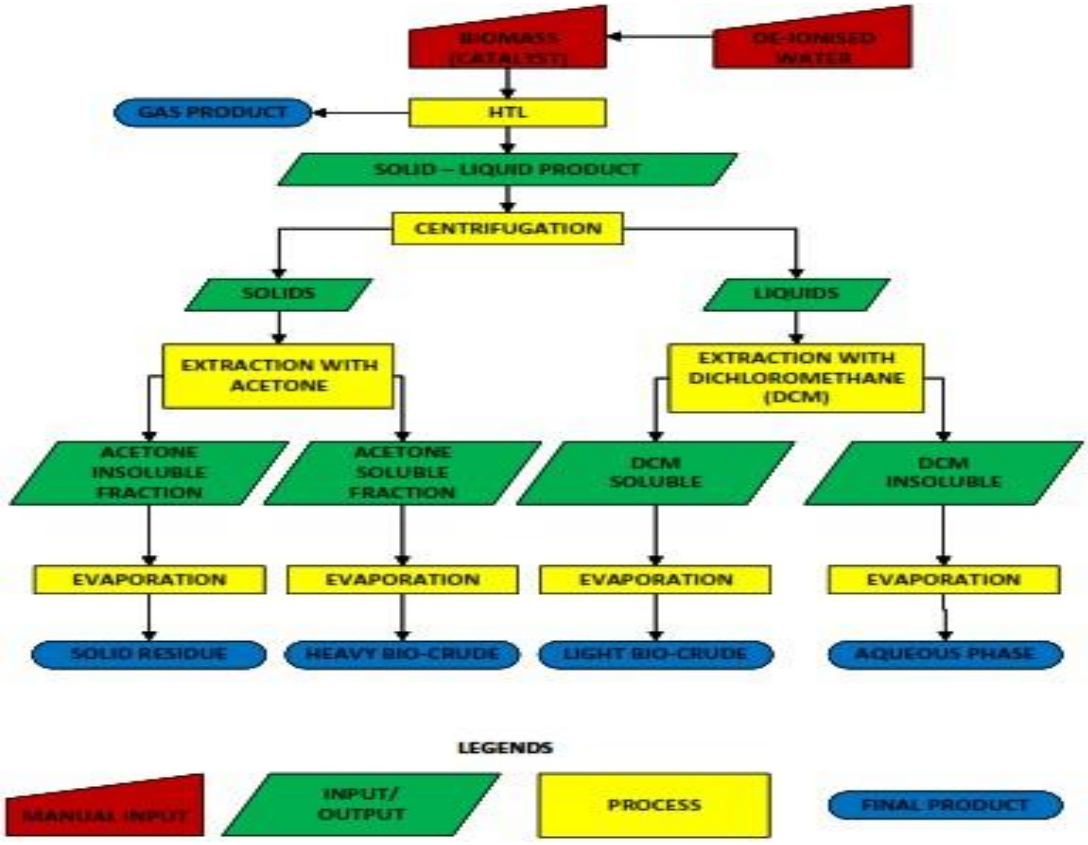


Figure 1: Scheme of product separation

A rough overall reaction pathway of MSK can be represented in Equation 6:

$$Biomass \rightarrow Biocrude + Gases + Aqueous\ Organics + Solid\ Residue\ (Char) \quad \ldots (6)$$

The yield of each product /fraction was defined in equation 7:

$$y_o = \frac{m_o}{M} \times 100 \quad \ldots (7)$$

Where M is the initial mass of the MSK sample, m is the mass of the products and y is the product yield. The subscript o refers to the liquid and solid phase products as well as the HBC and LBC.

RESULTS AND DISCUSSION

Distribution and yield of the product

The result of the Hydrothermal Liquefaction of Mango seed kernel across different temperatures (275°C, 300°C and 325°C) and reaction time (15, 30 and 45 mins) at a constant biomass to water ratio of 1:7 to evaluate its impact on product distribution is presented in Figure 2. The result showed that both temperature and residence time affect product yield. At 275°C 15mins, it was observed that the biocrude oil yield was at 24,2 wt%. The yield steadily increased as the reaction time increases. Increasing the temperature to 300°C, the yield also increases. At 300°C 15mins, the biocrude oil yield was at 26.1 wt%. No much increase was observed at 30mins and 45mins. When the temperature was increased to 325°C, the biocrude oil yield dropped to 19.9 wt% for 15mins. The yield further decreased to 19.5 wt% at 45mins.

The maximum biocrude oil yield is at 300°C for 30 mins which gives a 27.75 wt%. This aligns with findings by Yang et al (2021) which reported that HTL conditions typically between 280-320°C gives maximum oil yield from hemi-cellulosic biomass due to effective depolymerization and recombination of organic intermediates into oily compounds.

Conversely, at 325°C for 25 mins resulted in the lowest yield of about 19.5 wt%. It suggests that higher temperatures may not be conducive for measuring bio-oil yield in HTL process. The decrease in bio-oil yield as the temperature increases to 325°C with longer residence time may indicate thermal degradation which will favor mainly gas formation over bio-oil (Couto et al., 2017). Even Martins-Vieira et al., (2023) argued that higher temperatures break down organic matter further into gas during HTL process. Achieving higher yields at lower temperature comes with immense benefits both environmentally and economically. Operating at lower temperatures decreased energy consumption and enhances the efficiency of the energy conversion process (Gollakota et al., 2018).

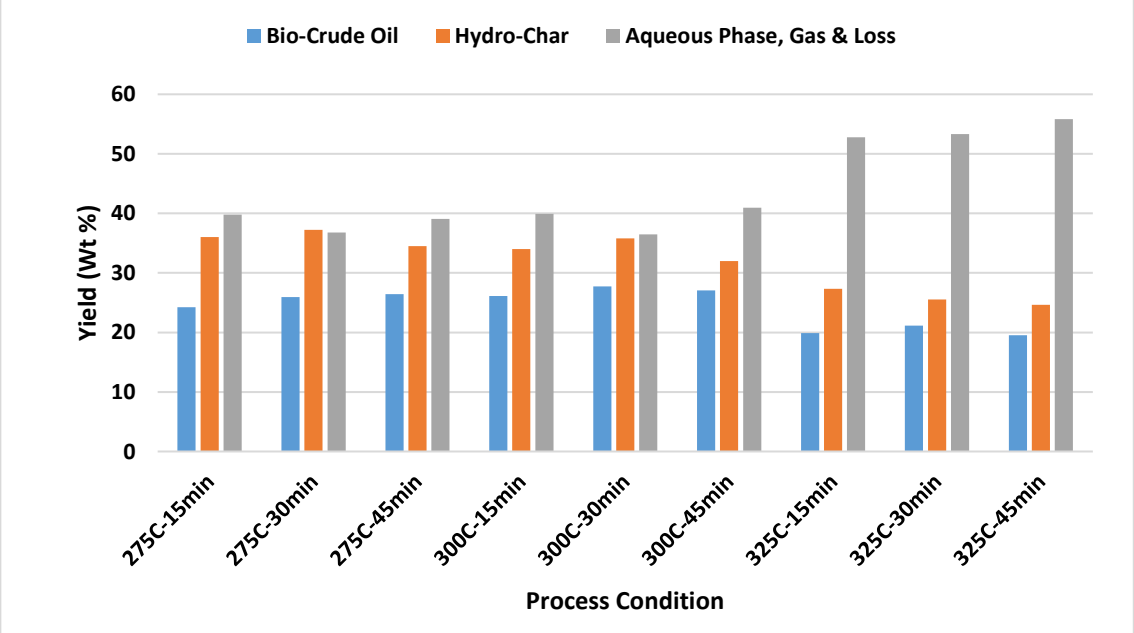


Figure 2: Distribution and yields (a) Biocrude Oil (b) Hydro-char (c) Aqueous phase, Gas & Loss products at different reaction temperatures and residence time

However, it was observed during the HTL process experiment that waxy products were formed at room temperatures after product separation. This arises due to the process taken place at lower temperatures or with short residence time. Biomass is not fully broken down, leading to intermediate products (Elliot et al., 2015). At lower residence time and sub-optimal temperature, the decomposed intermediates polymerize and recombine to form waxy fractions (Toor et al., 2011). But at higher temperature (325°C) and longer residence time (45 mins). The products decomposed and became stable.

The yield distribution of hydro-char indicates that at 275 °C, hydro-char was the dominant product fraction, achieving 37 wt% in 30 minutes. When the temperature rose to 300 °C, the hydro-char yield gradually fell to approximately 32 wt%. At 325°C, the yield of hydro-char decreased even more to 27 wt%. The high yield at 275 °C indicates insufficient depolymerization and dehydration of lignocellulosic components. Comparable behavior has been observed in HTL of different lignocellulosic feedstocks, where lower reaction conditions promote char production (Shahbeik et al., 2023). The decline at 300°C corresponds to the onset of hydrolysis and decarboxylation reactions in hemicellulose and lignin fractions, which are known to generate phenolics and other oil-soluble compounds (Zhuang et al., 2021). The further drop in hydro-char yield at 325°C suggests that higher

HTL conditions promote secondary depolymerization, solubilization, and gasification reactions (Jatoi et al., 2022).

In Figure 3, it is observed that the yield is more on the heavy biocrude than the light biocrude due to the reason that the lignin fragments tend to form large, aromatic and oxygenated compounds that are resistant to depolymerization (Yang et al., 2021).

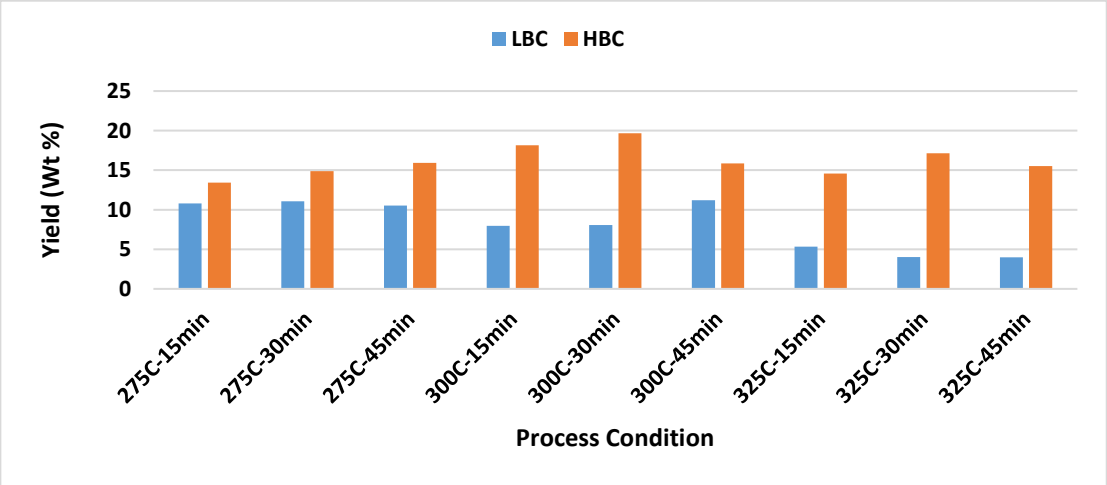


Figure 3: Fractions of (a) HBC and (b) LBC, which sum up to the yield of biocrude product at different temperature and residence time

The properties of biocrude oil

Functional group of the biocrude oil (light)

Figure 4 shows the FTIR spectrum, it reveals the functional group and fingerprints of the light biocrude oil from MSK HTL. The band at 3337cm^{-1} represents a broad, strong band which indicates hydrogen bonded O-H group. This usually reflects phenolic compounds and carboxylic acids derived from cellulose/hemicellulose decomposition in HTL light biocrudes. Bands around 1638 cm^{-1} is a C=O (carbonyl) stretch indicating the presence of esters which are typical of seed kernels. At bands 1459 cm^{-1} and 1364 cm^{-1} indicates an O-H(fingerprints) bending, COO-stretches which contains carboxylate. The FTIR of the light biocrude shows clear signature of oxygenated organics consistent with a low molecular weight, oxygen rich bio-oil containing acids, esters and relatively fewer highly condensed aromatics (Tahir et al., 2020).

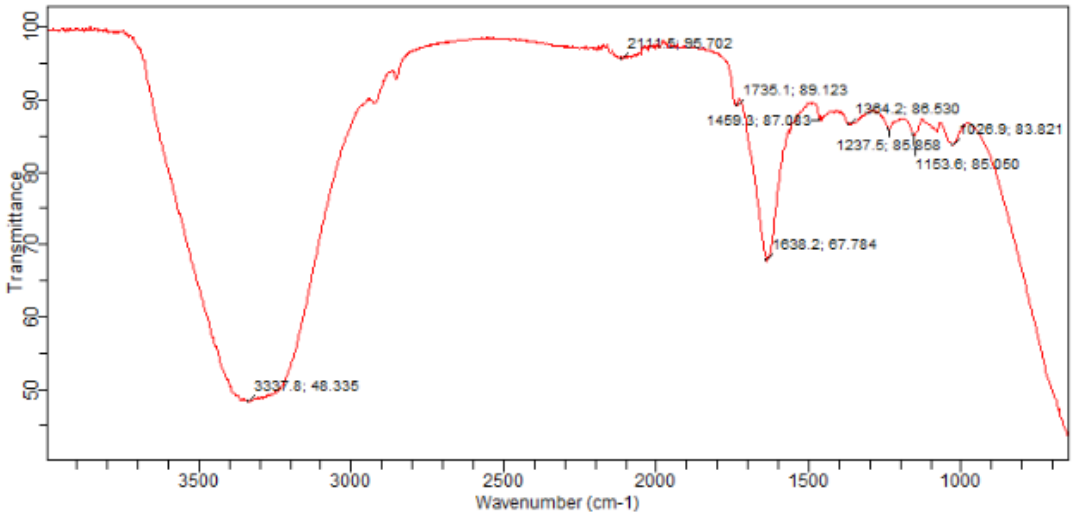


Figure 4: FTIR Spectra of Light biocrude oil

Functional group of the biocrude oil (heavy)

Figure 5 is the FTIR spectrum of the heavy biocrude of MSK. At band 3300 $cm^{-1}$is also an O-H stretching (narrower than light biocrude) which still indicates presence of carboxylic acids and phenols. At band 1638 cm^{-1} is a strong C=O which indicates carbonyl functionality. This suggests the presence of multiple carbonyl environments such as esters, carboxylic acids and ketones. At band 2883 cm^{-1} are aliphatic C-H stretching. This band maybe present but oftentimes reduced relative intensity compared with the light fraction reflecting loss of light aliphatic species or their incorporation into larger structure (Rizzo & Chiaramonti, 2022),

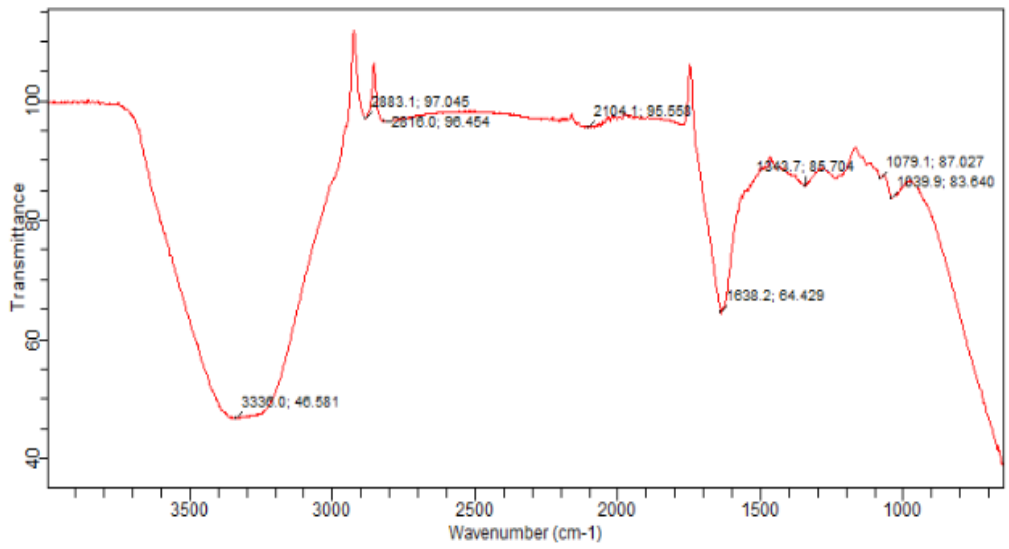


Figure 5: FTIR Spectra of Heavy biocrude oil

Major component of the biocrude oil

The GC-MS of the light and heavy biocrude reveals a diverse range of biocrude functional group as shown in Figure 6. The light biocrude is composed of cyclic compounds, carboxylic acids/esters, ketones, nitrogen containing compounds and aromatic compounds. Carboxylic acids/esters make up a great fraction of the GC-MS analysis signifying a high potential for biocrude production. The compounds are common in HTL of lipid rich biomass which are precursors to bio-fuel which is similar to findings by Akhtar & Amin (2011), in which they reported high lipid derivatives in HTL oils from agricultural waste. Nitrogen containing compounds are found which can be as a result of protein degradation under hydrothermal conditions (Biller and Rios, 2011). Aromatic and cyclic compounds can be due to the lignin decomposition of the seed kernel. They enhance fuel quality (Peterson et al., 2018). These compounds are promising for biofuel applications. The high carboxylic acid/ester content is particularly good for producing liquid biofuels or chemicals. Table 3 presents the list of chemicals derived from the light biocrude of the HTL process. Dominant compounds in the light biocrude consist of n-Hexadecanoic acid, 1,2-Benzenedicarboxylic acid, butyl 2-ethylhexyl ester and Bis(2-ethylhexyl) phthalate.

Table 3: List of Chemicals, retention time (RT) and percentage area of light biocrude oil derived from HTL process of MSK

No.	RT	Chemicals	Formular	%
1.	13.8404	Pentadecanoic acid, 14-methyl-, methyl ester	$C_{17}H_{34}O_2$	1.2178
2.	14.6597	1,2-Benzenedicarboxylic acid, butyl 2-ethylhexyl ester	$C_{20}H_{30}O_4$	8.6171
3.	14.8595	n-Hexadecanoic acid	$C_{16}H_{32}O_2$	7.1119
4.	16.5733	13-Octadecenal, (Z)-	$C_{18}H_{34}O$	1.2006
5.	17.7195	9-Octadecenoic acid (Z)-, 2,3-dihydroxypropyl ester	$C_{21}H_{40}O_4$	3.4155
6.	17.8452	Pentanoic acid, 10-undecenyl ester	$C_{16}H_{32}O_2$	1.3272
7.	17.9768	E-11-Hexadecenoic acid, ethyl ester	$C_{18}H_{34}O_2$	1.8214
8.	18.1554	Succinic acid, dodec-2-en-1-yl cis-pent-2-en-1-yl ester	$C_{21}H_{36}O_4$	1.3785
9.	23.7979	Bis(2-ethylhexyl) phthalate	$C_{24}H_{38}O_4$	64.5967
10.	28.8067	trans-2,3-Methylenedioxy-b-methyl-b-nitrostyrene	$C_{10}H_9O_4$	1.4125

Compounds emanating for the analysis of the heavy biocrude also consist primarily of carboxylic acids/esters and aromatic compounds. The carboxylic acids/esters are common bio-oil constituents gotten from thermal degradation and esterification of lipids during HTL. The fuel like properties of the biocrude is contributed by these compounds. Aromatics are found in the heavy biocrude as a result of secondary reactions of intermediates like phenol. They increase the energy content of the biocrude (Biller and Reiss, 2011). Table 4 list the chemicals found in the heavy biocrude. These include Phthalic acid, butyl isohexyl ester, 7,10,13-Hexadecatrienoic acid, methyl ester and also Bis(2-ethylhexyl) phthalate

Table 4: List of Chemicals, retention time (RT) and percentage area of light biocrude oil derived from HTL process of MSK

No.	RT	Chemicals	Formular	%
1.	3.7767	Dodecyl nonyl ether	$C_{21}H_{44}O$	0.6871
2.	3.9228	Naphthalene	$C_{10}H_8$	0.5821
3.	14.4058	Phthalic acid, butyl isohexyl ester	$C_{18}H_{26}O_4$	9.1949
4.	14.7275	Undecanoic acid, ethyl ester	$C_{12}H_{24}O_2$	1.3073
5.	17.333	trans-13-Octadecenoic acid	$C_{18}H_{34}O_2$	1.8386
6.	17.4936	9,12-Octadecadienoic acid, ethyl ester	$C_{20}H_{36}0_2$	1.2343
7.	17.5714	Ethyl Oleate	$C_{20}H_{38}O_2$	1.2253
8.	17.6419	7,10,13-Hexadecatrienoic acid, methyl ester	$C_{17}H_{38}O_4$	2.5259
9.	23.7279	Bis(2-ethylhexyl) phthalate	$C_{24}H_{38}O_4$	78.9912
10.	28.7858	MDMA methylene homolog	$C_{12}H_{17}NO_2$	0.3625

Chemicals such as Pentadecanoic acid, 14-methyl-, methyl ester, n-Hexadecanoic acid and Succinic acid, dodec-2-en-1-yl cis-pent-2-en-1-yl ester are considered green chemical precursors for biofuels (biodiesel, jet fuel), biodegradable, surfactants and lubricants, green solvents, biopolymers and plasticizers. Long chain fatty acids (trans-13-Octadecenoic acid) in the heavy biocrude can be used for bioplastics and cosmetics. Long-chain ethers in the heavy biocrude like dodecyl nonyl ether are used as green surfactant intermediates

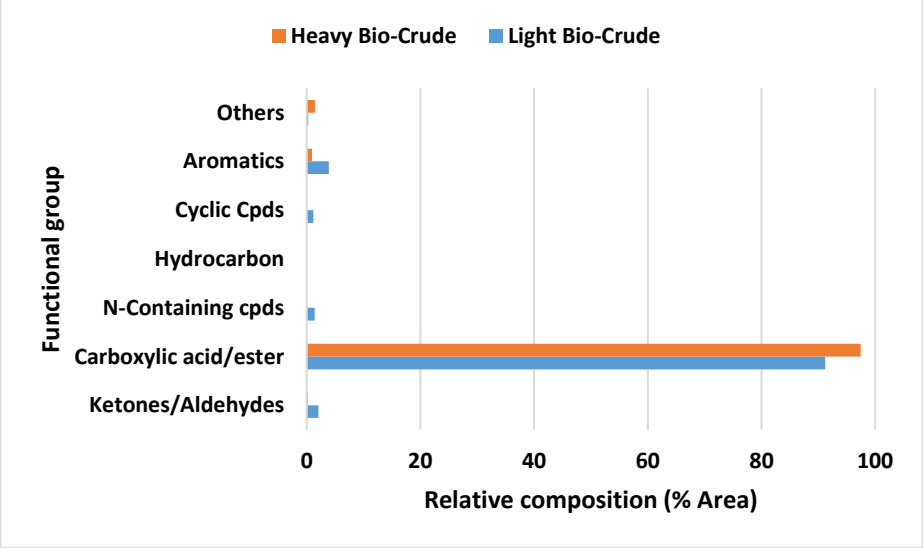


Figure 6: Functional groups of Biocrude Oil from MSK

Functional group of the hydro-char

FTIR analysis was used to identify the characteristic functional groups on the surface of the hydro-char. From the FTIR spectra in Figures 7, it can be seen that many peaks exist, indication of many functional groups on the surface of the hydro-char. Broad O-H at 3200-3600cm^{-1} which indicates hydrogen-bonded hydroxyls from phenolic and carboxylic groups in the char surface. At peaks around 2920, 2855 cm^{-1}, a limited residual aliphatic C-H chain. At peaks around 1700, 1620 and 1592 cm^{-1} points to conjugated carbonyls and aromatic ring C=C. The spectrum indicates a carbon-rich, increasingly aromatic hydro-char with oxygenated surface groups. The abundant surface oxygen functional groups can act as reactive anchors in catalytic upgrading routes, facilitating deoxygenation and ring hydrogenation to produce syngas and aromatic hydrocarbons (Madhusudhan et al., 2025).

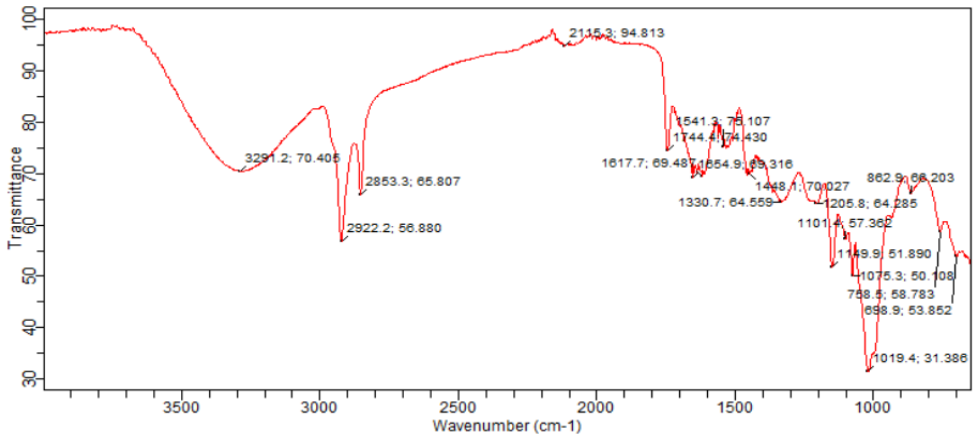


Figure 7: FTIR Spectra of Hydro-char

SEM analysis of the hydro-char

Scanning Electron Microscopy under 16500 magnification was used to determine the surface morphology and microporous structure of the hydro-char. Figure 8 shows the SEM of hydro-char at two representative spots (spot 1 and 5). As seen from the Figure, it shows an irregular, fixed carbonaceous particles with evolving meso-/microporosity suggesting a heterogeneous morphology. This heterogeneous morphology suggests the potential for pore development upon activation, making the hydro-char a suitable precursor for porous carbon materials used in adsorption, catalysis and as solid fuel (Suhas et al., 2025).

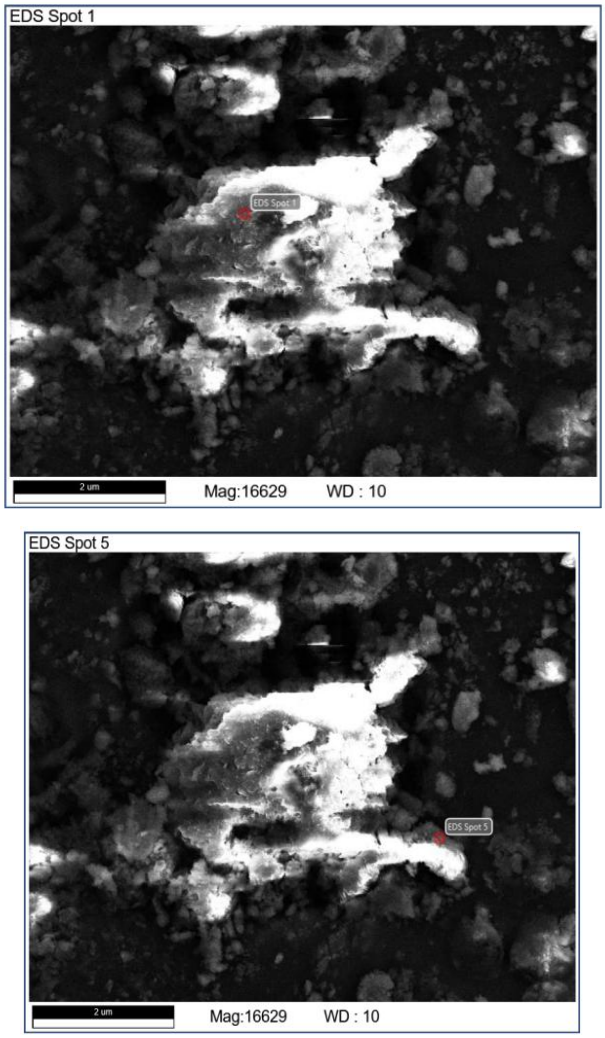


Figure 8: SEM images of hydro-char

EDS analysis of the hydro-char

An electron dispersion spectrophotometric analysis was carried out to determine the elemental content. The various elements present and their compositions are presented in Table 5 at the 2 different spots (spot 1 and 5). As seen from the Table, at spot 1, the carbon has the highest weight percentage composition at 80.79%, oxygen 18.66%, traces of Mg=0.16%, P=0.08%, S=0.09% and K=0.22%. At spot 5, the carbon is at 75.46%, O=24.23% and traces of other elements at 0.3% total. The dense C (75-81 wt%) with substantial O (19-24 wt%) is typical of HTL chars that form via dehydration and decarboxylation. Hydro-chars retain oxygenated groups after HTL. The carbon rich hydro-char can be used to catalyse dehydration and aromatization during thermochemical processing (Chen et al., 2024).

Table 5: Elemental analysis of hydro-char

Element	Weight %	
	Spot 1	Spot 5
C	80.79	75.46
O	18.66	24.23
Mg	0.16	0.07
P	0.08	0.03
S	0.09	0.11
K	0.22	0.09

Possible reaction pathways

Due to the varying reactions of chemical components involved in the HTL process, multiple potential reaction pathways for the HTL of organic biomass waste have been documented. It is challenging to detail all the reactions that occur since the reaction pathways can be intricate with limitless possibilities. Nonetheless, in this study, the biocrudes analysed by GCMS identified many compounds. This contributed to a deeper comprehension of the reaction network linking the chemical products derived from the MSK feedstock and is also tied to the FTIR bands.

The lipids in the MSK were mostly triglycerides. They underwent hydrolysis to fatty acids and glycerol as depicted in equation 8(Changi et al., 2012). This is supported by the FTIR O-H(3200-3600cm^{-1}) and a strong C=O of carboxylic acids and the free fatty acids (n-hexadecanoic acids, 7.11%) detected.

$$TAG\ (triacylglycerol) + 3H_2O \rightarrow glycerol + 3RCOOH \quad \ldots(8)$$

Fatty acids also underwent subsequent esterification with carbonyl intermediates to produce ester compounds depicted in equation 9 (Shah et al., 2022).

$$R - COOH + ROH \leftrightarrow R - COOR + H_2O \quad \ldots(9)$$

MSK contains carbohydrates that is hydrolyzed to glucose as oxygenates consistent with sugar such as 2H-pyran species are derived. Glucose degrades by three pathways. Dehydration to furans and furfural compounds. The second pathway is the decomposition of carbohydrates and formation of short-chain unsaturated intermediates. The third decomposition pathway is the production of Maillard products such as 2-(1-naphthyliminomethyl)-pyrrole derived in the oil (Shah et al., 2022).

CONCLUSION

Hydrothermal liquefaction of mango seed kernel is a viable method for converting agro-waste into biocrude oil, hydro-char and other value-added products. Among the tested conditions, 300°C for 30 minutes offered the highest oil yield. According to GC-MS analysis, chemicals such as Pentadecanoic acid, 14-methyl-, methyl ester and n-Hexadecanoic acid are considered green chemical precursors for biofuel (jet fuel, diesel), lubricants and green solvent. Long chain fatty acids like trans-13-Octadecenoic acid derived from the heavy biocrude can be used for cosmetics. The analytical results from the hydro-char embodies the key structural and compositional features favorable for conversion into bio-catalytic materials, energy-rich intermediates and chemical precursors. The study provides a foundational understanding of mango seed kernel behavior under hydrothermal liquefaction and highlights its potential as a precursor for biofuel and chemicals.

REFERENCES

Chen, J., Zhou, J., Zheng, W., Leng, S., Ai, Z., Zhang, W., Yang, Z., Yang, J., Xu, Z., Cao, J., Zhang, M., Leng, L., & Li, H. (2024). A complete review on the oxygen-containing functional groups of biochar: Formation mechanisms, detection methods, engineering, and applications. *The Science of the Total Environment*, *946*, 174081. https://doi.org/10.1016/j.scitotenv.2024.174081

Cheng, F., Bayat, H., Jena, U., and Brewer, C. E. (2020). Impact of feedstoccomposition on pyrolysis of low-cost, protein-and lignin-rich biomass: review. J. Anal. Appl. Pyrolysis 147:104780. doi: 10.1016/j.jaap.2020.104780

Couto, E. A., Pinto, F., Varela, F., Reis, A., Costa, P., & Calijuri, M. L. (2017). Hydrothermal liquefaction of biomass produced from domestic sewage treatment in high-rate ponds. *Renewable Energy*, *118*, 644–653. https://doi.org/10.1016/j.renene.2017.11.041

Divyabharathi, R., Subramanian, P (2022). Biocrude production from orange (*Citrus reticulata*) peel by hydrothermal liquefaction and process optimization. *Biomass Conv. Bioref.* **12**, 183–194. https://doi.org/10.1007/s13399-021-01383-3

Elliott, D. C., et al. (2015). Process development for hydrothermal liquefaction of algae feedstocks in a continuous-flow reactor. Algal Research, 2(4), 445–454. https://doi.org/10.1016/j.algal.2013.08.005

FAO, IFAD, UNICEF, WFP and WHO 2021 The State of Food Security and Nutrition in the World 2021. Transforming Food Systems for Food Security, Improved Nutrition and Affordable Healthy Diets for All (Rome: Food and Agriculture Organization of the United Nations) (https://doi.org/ 10.4060/cb4474en)

FAO 2021 World Food and Agriculture—Statistical Yearbook 2021 (Rome: Food and Agriculture Organization of the United Nations)

Gollakota, A. R. K., Kishore, N., & Gu, S. (2018). A review on hydrothermal liquefaction of biomass. Renewable and Sustainable Energy Reviews, 81, 1378–1392. doi:10.1016/j.rser.2017.05.178

Gu, Y., Zhang, X., Deal, B., Han, L., Zheng, J., and Ben, H. (2019). Advances in energy systems for valorization of aqueous byproducts generated from hydrothermal processing of biomass and systems thinking. Green. Chem. 21, 2518–2543. doi: 10.1039/C8GC03611J

Jatoi, A. S., Shah, A. A., Ahmed, J., Rehman, S., Sultan, S. H., Shah, A. K., Raza, A., Mubarak, N. M., Hashmi, Z., Usto, M. A., & Murtaza, M. (2022). Hydrothermal Liquefaction of Lignocellulosic and Protein-Containing Biomass: A Comprehensive Review. *Catalysts*, *12*(12), 1621. https://doi.org/10.3390/catal12121621

Jiang, Y., Yao, Y., Liu, H., Zhang, S., Bai, X., Ma, X., Wang, Y., & Ren, Q. (2023). Volatile organic compounds conversion pathways and odor gas emission characteristics in chicken manure composting process. *Frontiers in Ecology and Evolution*, *11*. https://doi.org/10.3389/fevo.2023.1192132

Maag, A., Paulsen, A., Amundsen, T., Yelvington, P., Tompsett, G., & Timko, M. (2018). *Catalytic Hydrothermal Liquefaction of Food Waste Using CeZrOx. Energies, 11(3), 564.* doi:10.3390/en11030564

Madhusudhan, A., Zelenka, T., Satrapinskyy, L., Roch, T., Gregor, M., Cheng, P., & Monfort, O. (2025). A comparative study of different activation methods for hydrochar: surface properties and removal of pharmaceutical pollutant in water. *Environmental Science and Pollution Research*. https://doi.org/10.1007/s11356-025-36706-8

Martins-Vieira, J. C., Lachos-Perez, D., Draszewski, C. P., Celante, D., & Castilhos, F. (2023). Sugar, hydrochar and bio-oil production by sequential hydrothermal processing of corn cob. *The Journal of Supercritical Fluids*, *194*, 105838. https://doi.org/10.1016/j.supflu.2023.105838

Rizzo, A. M., & Chiaramonti, D. (2022). Blending of Hydrothermal Liquefaction Biocrude with Residual Marine Fuel: An Experimental Assessment. *Energies*, *15*(2), 450. https://doi.org/10.3390/en15020450

Romo, C. (2019). Catalytic Hydrothermal Liquefaction of Food Waste: Worcester Polytechnic Institute

Shah, A. A., Sharma, K., Haider, M. S., Toor, S. S., Rosendahl, L. A., Pedersen, T. H., & Castello, D. (2022). The role of catalysts in biomass hydrothermal liquefaction and biocrude upgrading. *Processes*, *10*(2), 207. https://doi.org/10.3390/pr10020207

Shahbeik, H., Panahi, H. K. S., Dehhaghi, M., Guillemin, G. J., Fallahi, A., Hosseinzadeh-Bandbafha, H., Amiri, H., Rehan, M., Raikwar, D., Latine, H., Pandalone, B., Khoshnevisan, B., Sonne, C., Vaccaro, L., Nizami, A., Gupta, V. K., Lam, S. S., Pan, J., Luque, R., . . . Aghbashlo, M. (2023). Biomass to biofuels using hydrothermal liquefaction: A comprehensive review. *Renewable and Sustainable Energy Reviews*, *189*, 113976. https://doi.org/10.1016/j.rser.2023.113976

Shen, Y. (2024). Biomass pretreatment for steam gasification toward H_2-rich syngas production-An overview. *International journal of Hydrogen Energy*, (66), 90-102.

Suhas, N., Chaudhary, M., Chaudhary, S., Chaubey, S., Da Paixão Cansado, I. P., Dehghani, M. H., Tyagi, I., & Gaur, R. (2025). Transforming Biomass Waste into Hydrochars and Porous Activated Carbon: A Characterization Study. *Resources*, *14*(3), 34. https://doi.org/10.3390/resources14030034

Tahir, M. H., Cheng, X., Irfan, R. M., Ashraf, R., & Zhang, Y. (2020). Comparative chemical analysis of pyrolyzed bio oil using online TGA-FTIR and GC-MS. *Journal of Analytical and Applied Pyrolysis*, *150*, 104890. https://doi.org/10.1016/j.jaap.2020.104890

Toor, S. S., Rosendahl, L., & Rudolf, A. (2011). *Energy*, 36(5), 2328–2342

United Nations Environment Programme 2021 Food Waste Index Report 2021 (Nairobi)

Xuesong Liu, Jun Shen, Yun Guo, Sha Wang, Bin Chen, Lei Luo, Hai Zhang. Technical progress and perspective on the thermochemical conversion of kitchen waste and relevant applications: A comprehensive review. *Fuel* **2023**, *331,* 125803. https://doi.org/10.1016/j.fuel.2022.125803

Yang, J., Hong, C., Xing, Y., Zheng, Z., Li, Z., Zhao, X., & Qi, C. (2021). Research progress and hot spots of hydrothermal liquefaction for bio-oil production based on bibliometric analysis. *Environmental science and pollution research international*, *28*(7), 7621–7635. https://doi.org/10.1007/s11356-020-11942-2

Zhuang, X., Liu, J., Wang, C., Zhang, Q., & Ma, L. (2021). A review on the stepwise processes of hydrothermal liquefaction (HTL): Recovery of nitrogen sources and upgrading of biocrude. *Fuel*, *313*, 122671. https://doi.org/10.1016/j.fuel.2021.122671